Nuclear Instruments and Methods in Physics Research A 1069 (2024) 169875

Contents lists available at ScienceDirect

Nuclear Inst. and Methods in Physics Research, A

journal homepage: www.elsevier.com/locate/nima

Advancements in experimental techniques for measuring dipole moments of short-lived particles at the LHC

N. Neri [a,c,1,*], K. Akiba [b], F. Alessio [c], L. Bandiera [d], M. Benettoni [e], R. Cai [c], R. Cardinale [f], S. Cesare [a], M. Citterio [a], V. Coco [c], P. Collins [c], E. Dall'Occo [g], D. De Salvador [e], K. Dewhurst [c], M. Ferro-Luzzi [c], A. Fomin [h], R. Forty [c], J. Fu [i], P. Gandini [a], M.A. Giorgi [j], J. Grabowski [k], V. Guidi [d], P. Hermes [c], S.J. Jaimes Elles [l], S. Jakobsen [c], E. Kou [h], G. Lamanna [j], H.B. Li [i,m], S. Libralon [l], C. Maccani [c,e], L. Malagutti [d], D. Marangotto [a], F. Martinez Vidal [l], J. Mazorra de Cos [l], A. Mazzolari [d], A. Merli [a,2], H. Miao [i,m], D. Mirarchi [c], R. Negrello [d], S. Neubert [k], A. Petrolini [f], A. Pilloni [n], J. Pinzino [j], M. Prest [o], S. Redaelli [c], M. Romagnoni [d], P. Robbe [h], L. Rossi [a], J. Ruiz-Vidal [p], I. Sanderswood [l], A. Sergi [f], G. Simi [e], M. Sorbi [a], M. Sozzi [j], E. Spadaro Norella [f], A. Stocchi [h], M. Tamisari [d], G. Tonani [a], T. Tork [a], A. Triossi [e], N. Turini [q], E. Vallazza [o], S. Vico Gil [l], Z. Wang [a], M. Wang [a], T. Xing [a], M. Zanetti [e], F. Zangari [a]

[a] *Università degli Studi di Milano and INFN, Sezione di Milano, Via Celoria 16, 20133, Milan, Italy*
[b] *Nikhef, Science Park 105, 1098 XG, Amsterdam, Netherlands*
[c] *CERN, Espl. des Particules 1, 1211, Meyrin, Switzerland*
[d] *Università degli Studi di Ferrara and INFN, Sezione di Ferrara, Via G. Saragat 1, 44122, Ferrara, Italy*
[e] *Università degli Studi di Padova and INFN, Sezione di Padova, Laboratori Nazionali di Legnaro, Via F. Marzolo 8, 35131, Padova, Italy*
[f] *Università degli Studi di Genova and INFN, Sezione di Genova, Via Dodecaneso 33, 16146, Genova, Italy*
[g] *Technische Universität Dortmund, August-Schmidt-Str. 4, 44227, Dortmund, Germany*
[h] *IJCLab, Rue Georges Clemenceau 15, 91400, Orsay, France*
[i] *University of Chinese Academy of Sciences, Yuquan Road 19A, 100049, Beijing, China*
[j] *Università di Pisa and INFN, Sezione di Pisa, Largo B. Pontecorvo 3, 56127, Pisa, Italy*
[k] *University of Bonn, Nussallee 14-16, 53115, Bonn, Germany*
[l] *IFIC - Universitat de Valencia-CSIC, C/ Catedrático José Beltrán 2, 46980, Valencia, Spain*
[m] *Institute of High Energy Physics, Chinese Academy of Sciences, Yuquan Road 19A, 100049, Beijing, China*
[n] *Università degli Studi di Messina and INFN, Sezione di Catania, Piazza Pugliatti 1, 98122, Messina, Italy*
[o] *Università degli Studi dell'Insubria and INFN, Sezione di Milano Bicocca, Via Castelnuovo 7, 22100, Como, Italy*
[p] *Lund University, Professorsgatan 1B, 223 64, Lund, Sweden*
[q] *Università degli Studi di Siena and INFN, Sezione di Pisa, Via Roma 56, 53100, Siena, Italy*

ARTICLE INFO

Keywords:
Silicon detectors
Cherenkov detectors
LHC
Roman Pot

ABSTRACT

ALADDIN is a proposed fixed-target experiment at the LHC for the direct measurement of charm baryon dipole moments. The detector features a spectrometer and a Cherenkov detector, while the experimental technique is based on the phenomena of particle channelling and spin precession in bent crystals. TWOCRYST, a proof-of-principle test at the LHC for the proposed experiment, is planned during the LHC Run 3. Recent channelling efficiency measurements performed at the CERN SPS of bent crystals developed at INFN are presented, marking significant progress towards its realisation. The silicon pixel detector for TWOCRYST is under construction. It will work in the secondary vacuum of a Roman Pot positioned inside the LHC beam pipe. The design, construction and integration of the pixel detector inside the Roman Pot will be discussed, along with the design and perspectives for the proposed ALADDIN experiment.

* Corresponding author at: Università degli Studi di Milano and INFN, Sezione di Milano, Via Celoria 16, 20133, Milan, Italy.
E-mail address: nicola.neri@mi.infn.it (N. Neri).

[1] On behalf of the TWOCRYST collaboration and ALADDIN proto-collaboration.
[2] Now at EPFL, Lausanne, Switzerland.

https://doi.org/10.1016/j.nima.2024.169875
Received 4 July 2024; Received in revised form 2 September 2024; Accepted 9 September 2024
Available online 12 September 2024

1. Introduction

First direct measurements of Λ_c^+ and Ξ_c^+ charm baryon dipole moments have been proposed to be performed at the Large Hadron Collider (LHC) [1–7]. In the quark model $\Lambda_c^+ = [ud]c$ and $\Xi_c^+ = [us]c$, where the light quarks are in antisymmetric flavour functions, the magnetic dipole moment (MDM) of the baryons are the same as for the charm quark, $\boldsymbol{\mu}_{\Lambda_c^+} = \boldsymbol{\mu}_c$ and $\boldsymbol{\mu}_{\Xi_c^+} = \boldsymbol{\mu}_c$. An experimental confirmation of this relation plays an important role to test the quark model description. Theories beyond the quark model, such as heavy quark field theories, have provided predictions for magnetic dipole moments of the Λ_c^+ and the Ξ_c^+ baryons that could be tested with a measurement with 10% relative precision [8]. On the other hand, searches for electric dipole moments (EDM) of charm baryons would allow to probe for physics beyond the Standard Model (SM) [9]. According to simulations studies, first measurements of charm baryon dipole moments are possible in two years of data taking assuming a proton on target of 10^6 p/s on 2.0 cm thick W target, and non-negligible Λ_c^+ (Ξ_c^+) polarisation of about 0.25. A sensitivity on charm baryon MDM of $2 \cdot 10^{-2} \mu_N$ and on EDM of $3 \cdot 10^{-16}$ e cm with $1.4 \cdot 10^{13}$ protons on target is expected, where $\mu_N = e\hbar/2m_p$ is the nuclear magneton. The program of measurements include an exploration of the $g-2$ anomalous magnetic moment of the τ [10,11], and additional physics topics such as the measurement of charm hadron cross-sections and J/ψ photo-production in the very forward region at pseudorapidity $5 < \eta < 9$. This program of measurements and the machine layout have been studied within the Physic Beyond Collider working group at CERN [12].

2. Experimental technique

The charm baryon lifetimes are very short $\tau \approx 2-4 \times 10^{-13}$ s, therefore it is experimentally challenging to induce spin precession before their decay. The proposed experimental technique is based on a fixed-target experiment at the LHC, where 7 TeV protons impinge on a tungsten (W) target, at a centre-of-mass energy $\sqrt{s} \approx 110$ GeV. The idea is to exploit the phenomenon of channelling in bent crystals [13], for which positively charged particles entering the crystals with their momentum aligned with the atomic planes of the crystal gets trapped, and their transverse motion is confined by the crystal lattice potential well, corresponding to an interplanar electric field in silicon (Si) of about 6 GV/cm. Highly boosted charm baryons produced in pW collisions have an average Lorentz factor $\gamma \approx 900$, hence their flight length is relatively large, $\beta\gamma c\tau \approx 5$–10 cm. Channelled charm baryons travelling along the entire bent crystal are deflected along the direction defined by the crystal bending angle, θ_c, inside the detector acceptance. In addition, channelled baryons experience spin precession due to the interaction of their MDM/EDM with the intense electromagnetic field inside the crystal. The spin precession angle Φ is related to the gyromagnetic factor g, while the spin polarisation vector component perpendicular to the bending plane after the crystal, s'_x, is related to the gyroelectric factor d according to Eq. (1),

$$\Phi = \frac{g-2}{2}\gamma\theta_c, \qquad s'_x = s_0 \frac{d}{g-2}(\cos\Phi - 1). \tag{1}$$

The initial polarisation vector, s_0, is perpendicular to the production plane, defined by the incoming proton and the outgoing Λ_c^+ baryon momenta, for parity conservation in strong interactions. The final polarisation s' can be determined by an angular analysis of charm baryon decay products [7,14], where $|s'| = |s_0|$ since depolarisation in the bent crystal is negligible for channelled particles.

The signal event topology has two peculiar features: (i) the average momentum of the channelled charm baryons is very high, *i.e.* about 1.8 TeV/c for Λ_c^+ baryons for a bending angle $\theta_c = 7$ mrad; (ii) the direction in the bending plane of the channelled baryons is determined by the crystal bending angle. As a consequence, the momentum distribution of the decay products reaches 1.0 TeV/c and the angular distance between the charm baryon and the daughter particle momenta is $1/\gamma \approx 1$ mrad.

The proposed fixed-target experiment at LHC is based on a double-crystal setup designed and simulated by our machine colleagues [15]. The first crystal, the target collimator crystal for splitting (TCCS), has a bending angle of 50 μrad and is used to deflect protons from the beam halo towards a solid W target positioned about 100 m downstream of the TCCS. A second crystal, the target collimator crystal for precession (TCCP), with a bending angle of 7.0 mrad is positioned right after the W target. It induces spin precession to channelled charm baryons and deflects their trajectory within the acceptance of a forward detector to perform the reconstruction of signal decays. The proposed operational scenario is transparent to LHC high-intensity proton operations. A proof-of-principle (PoP) test at the LHC, the TWOCRYST project (see Fig. 1), has been approved for data taking in 2025 with the following objectives: (i) demonstrate the feasibility of the machine operations; (ii) confirm the achievable proton rate on target; (iii) measure the channelling efficiency at TeV energy using LHC protons; (iv) perform the necessary background studies to validate the simulations and the detector optimisation.

TCCS and TCCP bent crystals have been produced at INFN Ferrara according to the required specifications. They have been characterised on beam at the CERN H8 SPS in August 2023 using a 180 GeV/c positive hadron beam. The INFN tracking telescope features silicon strip sensors with 50 μm pitch to measure with 3.5 μrad accuracy the incoming angle of the hadrons impinging on the crystal. The silicon strip sensor positioned downstream of the crystal have 50 μm and 242 μm pitch to achieve an angular resolution of about 7.2 μrad on the outgoing angle of the tracks. A goniometer with 1 μrad accuracy for precision crystal alignment is used to achieve the conditions for channelling. Preliminary results report about 60% channelling efficiency for the TCCS and about 16% for the TCCP crystals. The offline analysis takes into account a potential mechanical torsion of the bent crystal that was measured to be about 20 μrad/mm. A detailed report of the testbeam results is currently in preparation [16].

3. The ALADDIN proposed experiment

The proposed experiment at LHC comprises two alternative scenarios: (i) a dedicated experiment at the insertion region 3 (IR3), the baseline scenario; (ii) the use of the LHCb detector at the interaction point 8 (IP8), kept as fallback option. The nominal solution at IR3, referred in the following with the acronym ALADDIN, "An Lhc Apparatus for Direct Dipole moments INvestigation", offers the advantage of an optimal detector design and particle identification information (PID) in the range of momenta up to 1 TeV/c. On the other hand, the construction of a new detector to be installed along the LHC tunnel will require significant resources and time for the design, construction, installation and commissioning. The LHCb based solution has the advantage of using an existing tracking detector and infrastructure, located in a equipped experimental area. On the other hand, the LHCb detector has no PID information for momenta greater than 100 GeV/c and the project could have potential interference with the LHCb core program and data taking. A tentative timeline of ALADDIN is the following: (i) proof-of-principle test during Run 3; (ii) construction and installation during the LHC Long Shutdown 3 (LS3); (iii) commissioning and data taking during Run 4. The region for the TWOCRYST PoP at IR3 has been identified and is being instrumented for operations in 2025. The same region is considered also suitable for the proposed ALADDIN experiment.

4. Detector developments

The detector layout for ALADDIN consists of a spectrometer and a Ring Imaging Cherenkov (RICH) detector (see Fig. 2). The spectrometer features pixel detectors positioned inside four Roman Pot (RP) stations,

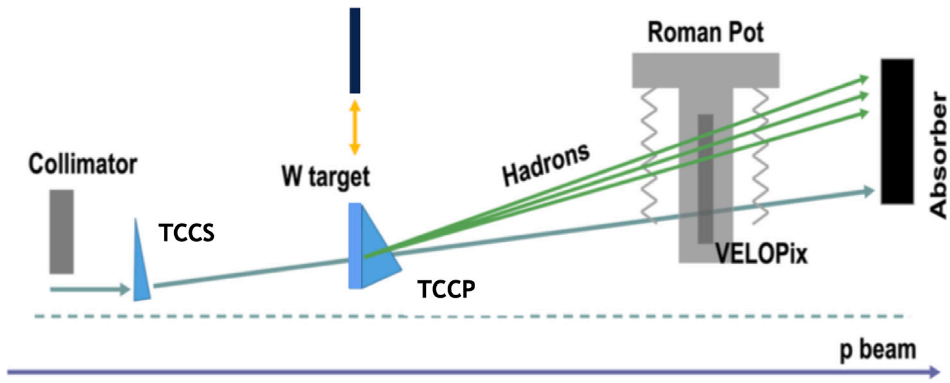

Fig. 1. Sketch of the TWOCRYST proof-of-principle test. LHC protons are deflected by the TCCS crystal towards the TCCP crystal and subsequently detected in the pixel detector housed in a Roman Pot to measure the channelling efficiency of the TCCP.

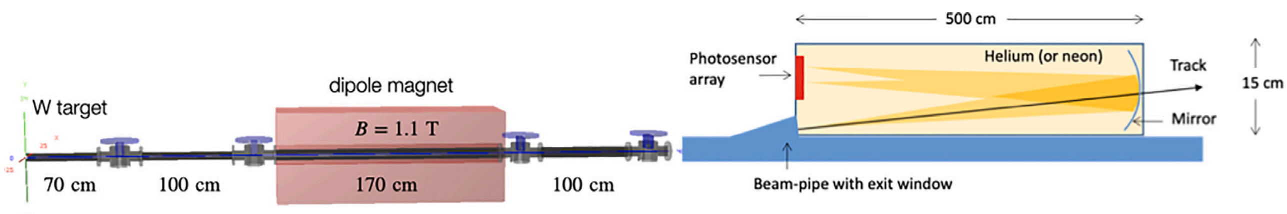

Fig. 2. ALADDIN detector side view. The spectrometer is on the left side and the RICH detector on the right.

and the Helium gas RICH detector is read out by a SiPM photosensor array. The length of the detector is approximately 10 m, with the spectrometer measuring around 4.4 m and the RICH measuring 5.0 m. The transverse dimension of the detector is confined within 1.0 m to fit into the available space along the LHC tunnel. The spectrometer features a warm dipole magnet, MCBWV.4L3.B2, available in situ, with a magnetic field of 1.1 T and an effective magnetic length of 1.7 m.

The specifications for the tracking detectors positioned upstream and downstream of the dipole magnet are reported in Table 1. The hit rates are estimated using full simulations. The hit rates on the RICH photosensors are expected to be relatively small since they are positioned 10 cm away from the beam and are outside of the detector acceptance. As alternative to the Si pixel sensors, Si strip sensors could be used for the downstream tracking stations but with reduced performance. The spectrometer is composed of four tracking stations, two upstream and two downstream of the dipole magnet, and has an acceptance in the very forward region, at pseudorapidity $5 < \eta < 9$. To achieve this, Si pixel sensors are housed inside RP stations and positioned inside the LHC beampipe. The spectrometer performance has been studied using full simulations based on DD4hep [17] for the description of the detector geometry and GEANT4 [18] for the simulation of the interaction of particles with the material. Physics collision events are generated using the PYTHIA8 Angantyr [19] model to account for pW interactions. The resolution for a charged particle with momentum $p = 500$ GeV/c is estimated to be $\frac{\sigma_p}{p} \approx \frac{2p}{0.3BLD}\sigma_x = 2\%$, where $BL = 1.9$ Tm is the magnet bending power, $D = 1.0$ m is the distance between two tracking stations, as shown in Fig. 2, and $\sigma_x = 10\ \mu\text{m}$ is the spatial resolution of the Si pixel sensors. The corresponding track angle resolution is estimated to be $\sigma_\theta \approx \sqrt{2}\sigma_x/D = 14\ \mu\text{rad}$, which is relevant to select channelled charm baryons exiting the crystal with the momentum direction determined by the crystal bending angle. The resolution on the impact parameter in the transverse plane is expected to be about 20 μm for high-momentum tracks. The acceptance for signal $\Lambda_c^+ \to pK^-\pi^+$ decays is studied as a function of the distance D between the tracking stations. The acceptance decreases when the distance D increases due to particles that are hitting the beampipe and exiting the detector acceptance. On the other hand, a large value of $D \approx 1.0$ m is beneficial for the momentum and track angle resolution. According to simulations, a resolution of 25 MeV/c^2 on the reconstructed invariant mass $m(pK\pi)$ is achievable for signal Λ_c^+ decays. An acceptance of about 70% or larger is achievable by enlarging the radius of the beampipe in the tracking volume and modifying the geometry of the present RPs. A potential future upgrade of the spectrometer considers the use of a compact dipole magnet in 20 K high-temperature superconducting (HTS) technology, with magnetic field $B = 4$ T and effective length $L = 1$ m. In this case, improvements in signal acceptance, reaching 90%, and in momentum resolution, about a factor of two, would become available.

4.1. Pixel sensor modules

The pixel detector of the spectrometer is based on the LHCb VELO pixel sensors and VeloPix ASIC [20]. The Si sensor is 200 μm thick and it is built in n-in-p technology. The pixel size is 55 μm and the sensor is organised in tiles with an area of 15×43 mm^2. Each sensor tile is readout by three VeloPix ASICs, connected to the sensor via bump-bonding. The VeloPix ASIC consists in a matrix of 256×256 pixels and is built in TSMC 130 nm CMOS technology, with radiation hardness greater than 4 MGy and tolerance to single-event upset. The maximum peak rate per pixel is 50 kHz and the data rate per ASIC is 20.48 Gbit/s, with an associated power consumption of about 1.2 W. The design of the pixel sensor module is shown in Fig. 3, which comprises the sensor tile, the data flex, and the GBTx chip, a bidirectional 4.8 Gb/s link between the radiation hard on-detector custom electronics and the off-detector systems. The aluminium base plate has good thermal conductivity and is connected to a cooling system based on a Peltier device positioned inside the RP to evacuate the power dissipated by the front-end electronics. The Peltier itself is connected to an external water circuit to exchange heat with a source external to the RP box. For the TWOCRYST detector, three pixel modules will be installed inside a RP station. The cooling sytem is designed to cope with 45 W power dissipation and guarantee a temperature of 20 °C for the sensors. A vacuum-feed-through board and a rigid-flex data cable have been designed to accommodate control and data lines inside the RP station and to connect with the optical and power board (OPB), whose main

Table 1
Specifications required for the tracking detectors positioned upstream and downstream of the spectrometer dipole magnet.

	Pitch (μm)	Hit rate (MHz/cm^2)	Dluence (n_{eq}/cm^2)	Area (cm^2)	Tech. solution
Upstream	55	250	3.5×10^{15}	10	Si pixel
Downstream	100	30	9.0×10^{13}	30	Si pixel/strip

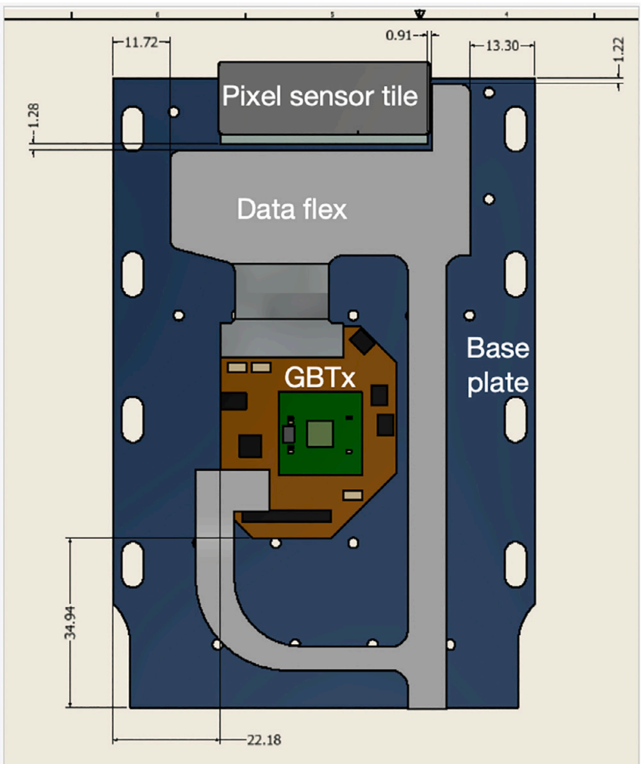

Fig. 3. Pixel sensor module developed for the TWOCRYST project. The dimensions reported in the sketch are in mm.

function is the optical–electrical conversion of the high-speed data and control signals that are sent to and from the detector module. An ATLAS-ALFA RP station has been extracted from the LHC tunnel and is made available to house the TWOCRYST pixel detector. The rectangular section of the pot is $128 \times 60 \times 46$ mm^3 (width × height × thickness). The RP also requires cooling due to the heating caused by the proton bunches passing in the cavity around the RP. A copper layer inside the box is used to bring the heat outside the RP.

4.2. RICH detector

A RICH detector is designed to identify protons, kaons and pions up to momenta of 1 TeV/c. The choice of helium radiator gas with refractive index $n = 1.000035$ and the length of the gas vessel of 5.0 m guarantee good separation power between the different particles at high momenta, and also provide a sufficient number of detected Cherenkov photons per track, $N_{pe} \approx 12$. The design takes inspiration from the NA62 RICH detector, based on 17 m long vessel filled with neon as radiator gas and readout by traditional photomultipliers (PMT). In this case, modern photosensors are considered with improved photon detection efficiency and finer granularity, *e.g.* silicon photomultipliers (SiPM) or micro channel plate PMT (MCP-PMT). The estimated angular resolution per photon on the Cherenkov angle is about 42 μrad, with contributions from chromatic dispersion (32 μrad), emission point uncertainty (6 μrad), and limited pixel granularity of the photosensor (30 μrad). The last contribution assumes a pixel size for SiPM of 0.5×0.5 mm^2, which requires some R&D in order to be used in the experiment. The photosensor area is relatively small, about 100 cm^2, keeping the transverse dimensions of the vessel limited to about 15 cm.

The pattern recognition of Cherenkov rings is relatively easy given the low occupancy of the photosensor detector, about 0.1%, with 38k channels. The upper limit for 3σ K-π and p-π separation is 610 GeV/c and 1.2 TeV/c, respectively. The PID performance has been studied with (without) the RICH using a simulated sample of $\Lambda_c^+ \to pK^-\pi^+$ decays for signal, and $D^+ \to K^-\pi^+\pi^+$, $D_s^+ \to K^+K^-\pi^+$ decays for background, achieving 90% signal retention for 95% (50%) background rejection.

5. Summary

Advancements in the experimental techniques for the measurement of charm baryon dipole moments have been presented. They include progress on machine aspects, construction and test of bent crystals, developments of detector and experimental techniques to perform the dipole moment measurements. A proof-of-principle test at LHC, the TWOCRYST project, has been approved for data taking in 2025 to demonstrate the feasibility of the future experiment. ALADDIN, is the proposed fixed-target experiment at LHC IR3 designed to perform the first direct measurements of charm baryon dipole moments. It features a spectrometer with pixel detectors housed in Roman Pots and a RICH detector for particle identification. A Letter of Intent is in preparation, aiming for data taking during LHC Run 4. [3]

Acknowledgements

We thank our colleagues in the CERN accelerator department for the fruitful collaboration, the colleagues of the LHCb VELO group for providing invaluable support for the pixel detector. We acknowledge support from CERN and from the national agencies: MOST and NSFC (China); CNRS/IN2P3 (France); BMBF, DFG and MPG (Germany); INFN (Italy); MICIU, AEI and GVA (Spain). We acknowledge financial support by the Italian Ministry of University and Research (MUR), Project Title 202277EWLW; the ERC Consolidator Grant SELDOM G.A. 771642; the NRRP - NextGeneration EU in the Valencian Community GVANEXT Project Reference ASFAE/2022/030.

References

[1] L. Burmistrov, et al., UA9, Measurement of Short Living Baryon Magnetic Moment using Bent Crystals at SPS and LHC, CERN-SPSC-2016-030, SPSC-EOI-012, 2016, URL: https://cds.cern.ch/record/2194564.

[2] V.G. Baryshevsky, The possibility to measure the magnetic moments of short-lived particles (charm and beauty baryons) at LHC and FCC energies using the phenomenon of spin rotation in crystals, Phys. Lett. B 757 (2016) 426–429, http://dx.doi.org/10.1016/j.physletb.2016.04.025, URL: https://www.sciencedirect.com/science/article/pii/S0370269316300983.

[3] F.J. Botella, et al., On the search for the electric dipole moment of strange and charm baryons at LHC, Eur. Phys. J. C 181 (2017) http://dx.doi.org/10.1140/epjc/s10052-017-4679-y, URL: https://link.springer.com/article/10.1140/epjc/s10052-017-4679-y.

[4] A.S. Fomin, et al., Feasibility of measuring the magnetic dipole moments of the charm baryons at the LHC using bent crystals, J. High Energy Phys. 120 (2017) http://dx.doi.org/10.1007/JHEP08(2017)120, URL: https://link.springer.com/article/10.1007/JHEP08(2017)120.

[3] At the time of the writing of this document the Letter of Intent has been presented [21].

[5] E. Bagli, et al., Electromagnetic dipole moments of charged baryons with bent crystals at the LHC, Eur. Phys. J. C 77 (2017) 828, http://dx.doi.org/10.1140/epjc/s10052-017-5400-x, URL: https://link.springer.com/article/10.1140/epjc/s10052-017-5400-x.

[6] A.S. Fomin, et al., The prospect of charm quark magnetic moment determination, Eur. Phys. J. C 80 (2020) 358, http://dx.doi.org/10.1140/epjc/s10052-020-7891-0, URL: https://link.springer.com/article/10.1140/epjc/s10052-020-7891-0.

[7] S. Aiola, et al., Progress towards the first measurement of charm baryon dipole moments, Phys. Rev. D 103 (2021) 072003, http://dx.doi.org/10.1103/PhysRevD.103.072003, URL: https://link.aps.org/doi/10.1103/PhysRevD.103.072003.

[8] A. Dainese, et al., [QCD Working Group], Physics beyond colliders: QCD working group report, 2019, http://dx.doi.org/10.48550/arXiv.1901.04482, arXiv:1901.04482, URL: https://arxiv.org/abs/1901.04482.

[9] J. Beacham, et al., Physics beyond colliders at CERN: beyond the Standard Model working group report, J. Phys. G: Nucl. Part. Phys. 47 (1) (2019) 010501, http://dx.doi.org/10.1088/1361-6471/ab4cd2.

[10] A.S. Fomin, et al., Feasibility of τ -lepton electromagnetic dipole moments measurement using bent crystal at the LHC, J. High Energy Phys. 03 (2019) 156, http://dx.doi.org/10.1007/JHEP03(2019)156, URL: https://link.springer.com/article/10.1007/JHEP03(2019)156.

[11] J. Fu, et al., Novel method for the direct measurement of the τ lepton dipole moments, Phys. Rev. Lett. 123 (2019) 011801, http://dx.doi.org/10.1103/PhysRevLett.123.011801, URL: https://link.aps.org/doi/10.1103/PhysRevLett.123.011801.

[12] C. Barschel, et al., LHC fixed target experiments : Report from the LHC fixed target working group of the CERN physics beyond colliders forum, CERN Yellow Reports: Monographs, vol. 4/2020, CERN, Geneva, 2020, http://dx.doi.org/10.23731/CYRM-2020-004, URL: https://inspirehep.net/literature/1802496.

[13] V.M. Biryukov, et al., Crystal Channeling and Its Application at High-Energy Accelerators, Springer-Verlag Berlin Heidelberg, 1997, http://dx.doi.org/10.1007/978-3-662-03407-1, URL: https://link.springer.com/book/10.1007/978-3-662-03407-1.

[14] D. Marangotto, Extracting maximum information from polarised baryon decays via amplitude analysis: The $\Lambda_c \to pK\pi$ case, Adv. High Energy Phys. 2020 (2020) 7463073, http://dx.doi.org/10.1155/2020/7463073, URL: https://www.hindawi.com/journals/ahep/2020/7463073/.

[15] D. Mirarchi, et al., Layouts for fixed-target experiments and dipole moment measurements of short-lived baryons using bent crystals at the LHC, Eur. Phys. J. C 80 (10) (2020) 1–16.

[16] S. Cesare, et al., Performance of short and long bent crystals for the TWOCRYST experiment at the Large Hadron Collider (LHC), 2024, in preparation.

[17] M. Frank, et al., DD4hep: A detector description toolkit for high energy physics experiments, J. Phys.: Conf. Ser. 513 (2) (2014) 022010, http://dx.doi.org/10.1088/1742-6596/513/2/022010.

[18] S. Agostinelli, et al., (GEANT4), GEANT4 - a simulation toolkit, Nucl. Instrum. Methods A 506 (2003) 250–303, http://dx.doi.org/10.1016/S0168-9002(03)01368-8.

[19] C. Bierlich, et al., The Angantyr model for heavy-ion collisions in PYTHIA8, High Energy Phys. 134 (2018) http://dx.doi.org/10.1007/JHEP10(2018)134, URL: https://link.springer.com/article/10.1007/JHEP10(2018)134.

[20] R. Aaij, et al., (LHCb Collaboration), LHCb VELO Upgrade Technical Design Report, Technical Report, CERN, 2013, URL: https://cds.cern.ch/record/1624070.

[21] K. Akiba, et al., ALADDIN: An Lhc Apparatus for Direct Dipole moments INvestigation, CERN-LHCC-2024-011, LHCC-I-041, CERN, Geneva, 2024, http://dx.doi.org/10.17181/CERN.2G4V.0YAO, https://cds.cern.ch/record/2905467.